Investigation of the effects of pulse repetition frequency in a mixed electric field on a SDBD-like plasma jet

Amir Abbas Heidari, Pourya Seyfi, Ahmad Khademi, Hamid Ghomi*

Abstract
In this paper, the design, performance and characterization of a low temperature argon plasma jet with a Surface Dielectric Barrier Discharge (SDBD)-like structure are presented. Based on this structure, the argon plasma jet is generated in a SDBD-like structure with a mixed electric field. SDBD-like structure, refers to the plasma jet generated by the surface dielectric barrier discharge. The effects of high frequency electric pulse as the main igniter for plasma jet generation and low frequency sinusoidal electric field in order to modify the dynamic behavior of plasma jet are investigated in this paper. The effect of these variations on the plasma jet along with the decrease in pulse repetition frequency were recorded by Schlieren imaging method. This study revealed the important role of decreasing the pulse repetition frequency in the mixed electric field in the SDBD-like plasma jet structure. Increasing the cross-sectional area of the plasma colliding with the target surface is the most important advantage of this structure for the generation of plasma jets. Also, the trend of decreasing plasma column continuity with increasing pulse repetition frequency is another result of this study. Under these conditions, the diameter of the cross section of the plasma jet increases to 9 mm without increasing the consumption of more electrical power and with equal jet length. Finally, the surface hydrophilicity was measured after treatment by plasma jet and the operation resulted in a super-hydrophilic surface.

Keywords
Plasma jet, Surface dielectric barrier discharge (SDBD), Pulse repetition frequency, Hydrophilicity, Modulated electric Field.

1. Introduction

Today, plasma science is a leader in advanced science. With the advancement of plasma science, new instruments in this field are being designed for various applications [1–3]. Devices based on dielectric barrier discharge (DBD), surface dielectric barrier discharge (SDBD), atmospheric cold plasma jets (ACPJ) are developing rapidly in plasma applications [4–6].

In the last decade, using plasma jets in surface engineering has been the subject of intense research worldwide because of their special effects on the surface [7, 8]. Among the major applications of plasma jets, one can name the hydrophilicity and hydrophobicity of the surface, disinfection of surfaces, chemical activation of surfaces, and the creation of functional groups on the surface for specific applications. Several gases are used as the plasma generator given the plasma jet applications [9, 10].

Argon, helium, and air are among the most critical gases used in industry and biology to plasma generation [11, 12]. However, different conditions are needed in terms of electrical power, duty cycle, and pulse repetition frequency to provide the electrical energy required to create a plasma jet in each gas [13–15]. Another essential component in generating plasma jets is designing a jet nozzle [16]. Applying the power source and the mechanism of plasma generation in the plasma reactor has a great impact on plasma generation and increases the efficiency of plasma jet [17, 18]. As a result of accurate design, we achieve a plasma jet with an acceptable jet length and cross-sectional diameter. The cross-sectional area of the plasma jet colliding with the surface is an important parameter in surface processing [19]. Therefore, proposing any method to amplify the plasma jet will greatly assistance reduce the energy consumption and time required for surface treatment [20, 21]. For this purpose, in this article, we have used two techniques simultaneously. In the first step, a plasma jet nozzle with a surface dielectric barrier discharge (SDBD) design was utilized and this technique allowed us to have plasma jet as large as the inside diameter of the reactor during the plasma generation step. In the second stage, we used an external electric field to control the ionic wind generated by the SDBD, which led to the control and optimization of the plasma jet. Finally, by treating a standard steel surface by the generated plasma jet and varying the parameters of the
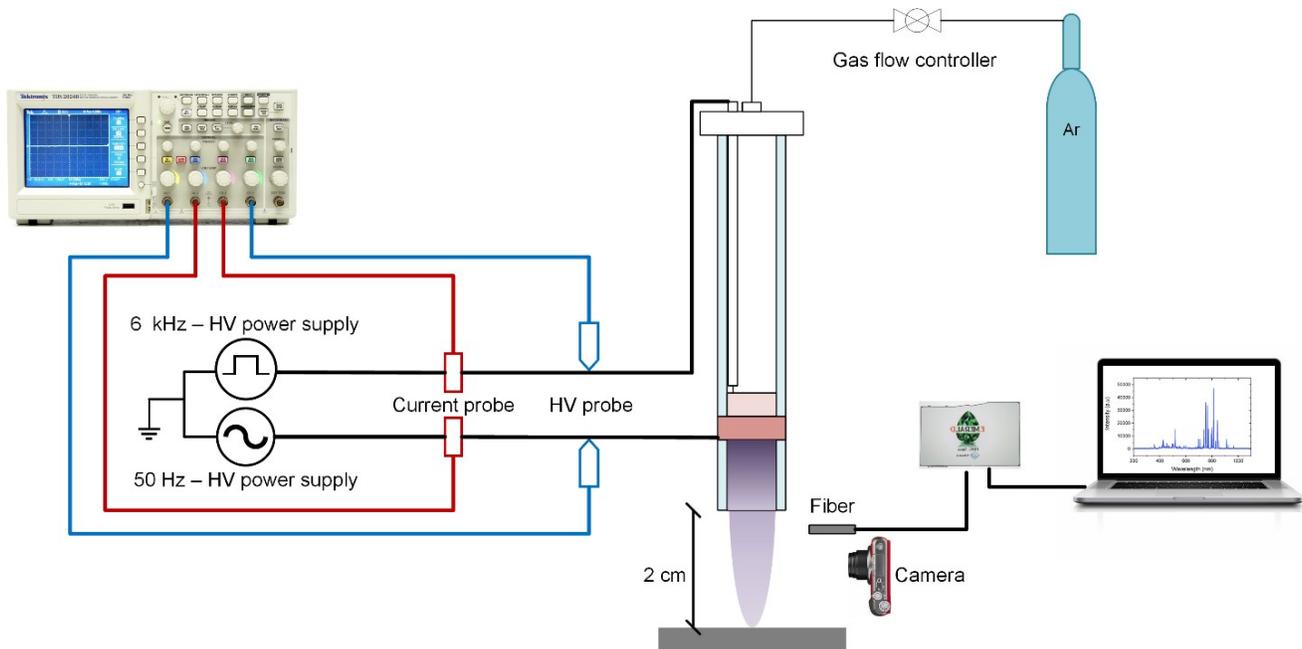
Figure 1. The schematic of the experimental SDBD-like plasma jet set-up and measurement tools.
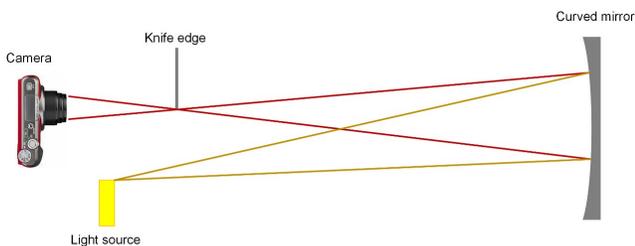
Figure 2. The schematics of single mirror-type schlieren setup and the argon plasma jet which is put in controlled condition in the front of the parabolic mirror.
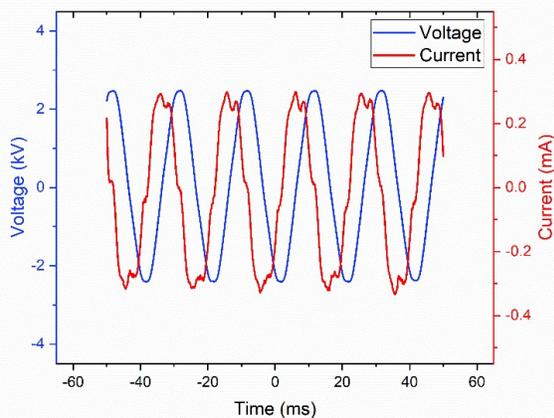
Figure 3. The voltage and jet current waveforms of 50Hz sinusoidal power supply used for the outer ring electrode.

plasma jet, we will parameterize the optimal conditions. Also, in characterizing plasma jet, schlieren method was used to parameterize the dynamic behavior of plasma jet. This method is an important technique in detecting and imaging variationes fluid current density.

2. Material and methods

A schematic of the experimental setup is shown in Figure 1. The SDBD like plasma jet consists of a quartz tube (inner diameter 9 mm, length 10 cm) and a copper ring-ring electrodes configuration. The rings have the same width and are equal to 2 cm. The outer electrode is located 2 cm from the end of the tube and connected to a 50 Hz sinusoidal power supply (Figure 3). A mid-frequency pulse power supply powered the inner electrode (Figure 4). The electrical power is transmitted to the internal electrode by a high voltage wire through the Teflon holder. Due to high voltage, for electric field modulation, we used a pulse modulation mechanism (an amplitude modulation type) [22]. Argon gas flowed through the quartz with a flow rate of 8 slm (standard liter per minute). A Casio Exilim Ex-ZR700 digital camera records the length of the plasma jet. The voltage and the current are measured by a high voltage probe (TEKTRONIX P6015 1:1000) and a Rogowski coil [23]. The electrical signals are visualized using a TEKTRONIX TDS 2024B oscilloscope (200 MHz). Schlieren photography was used to image the neutral gas flow ejected from a plasma jet. (Figure 2). The components of this setup are arranged in a single mirror configuration, described in detail in [24]. The optical emission spectrometer (OES) was used to detect plasma spectral. The optical fiber was placed 3 mm below the jet nozzle and 12 mm from its central axis. The average electrical power applied to the plasma jet with follow-
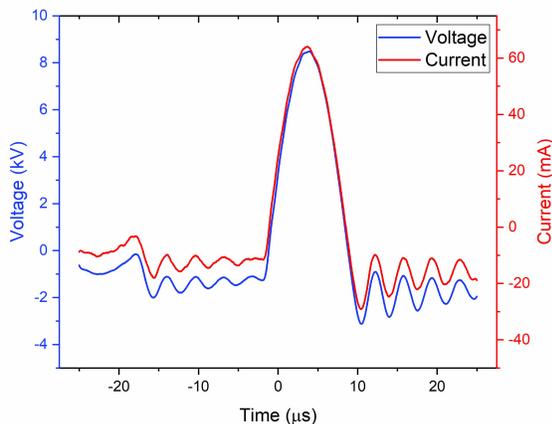
Figure 4. The voltage and jet current waveforms of pulsed power supply used for the internal ring electrode.

ing equations, where P_{ave} is average, $P(t)$ is time-dependent electrical powers, E_{pulse} is the energy per pulse, $V(t)$ and $I(t)$ are the time dependent voltage and current, respectively.

$$P(t) = V(t) \times I(t) \qquad (1)$$

$$E_{pulse} = \int_0^T P(t)dt \qquad (2)$$

$$P_{ave} = \frac{E_{pulse}}{T} \qquad (3)$$

$$P_{total} = P_{ave}(6KHz) + P_{ave}(50Hz) \qquad (4)$$

The total power consumption of two power supplies is shown by P_{total}. The total electrical power is assumed to be constant (25 watts) in all measurements and treatments. The power in the pulsed power supply is controlled by changing the duty cycle, and it is controlled by a current control resistor in the sinusoidal power supply. The plasma jet was irradiated onto the SUS304 stainless steel substrate (12×14 mm^2). The distance between the substrate and nuzzle is two centimeters. All treatments were performed on the surface in such a way that the potential of the substrate was floating. The surface was treated for 10 seconds by a plasma jet perpendicular to its center. The wettability of the substrate is quantified by water contact angle measurement. A static contact angle was measured using a sessile drop method.

3. Results and discussion

By applying a mixed electric field to a plasma jet nozzle, amplitude modulation(AM) in the applied electric field occurs at
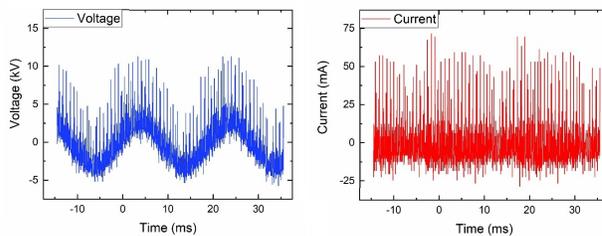
Figure 5. The voltage and jet current waveforms when both power supplies are applied simultaneously (Amplitude-Modulated power supply).

the site of electric discharge formation. As shown in the Figure 5, a high-frequency pulse is swept over a low-frequency voltage, forming a superwave. Examining the behavior of the plasma jet in the new structure (SDBD-like plasma jet), the formation of a plasma ring in a large diameter nozzle can be clearly seen. This behavior can be seen in schlieren images(Figure 7) in general conditions. Now, by varying the frequency of the igniter pulse, we will examine how the plasma jet column is formed. The result of these changes is reported in Figure 6. At first glance, you can see the increase in the diameter of the plasma jet and the increase in the length of the plasma jet. This amplification in the plasma jet is due to the effects of the S-DBD like structure as well as the effects of the bias voltage. At this stage, with a decreasing trend in the frequency of the pulse power supply, it was observed that by decreasing the frequency of repetition of the pulses in equal electrical power, we will have a more stable plasma jet at low frequency. In general, we obtained an acceptable plasma jet by using a SDBD-like plasma jet structure and also by applying
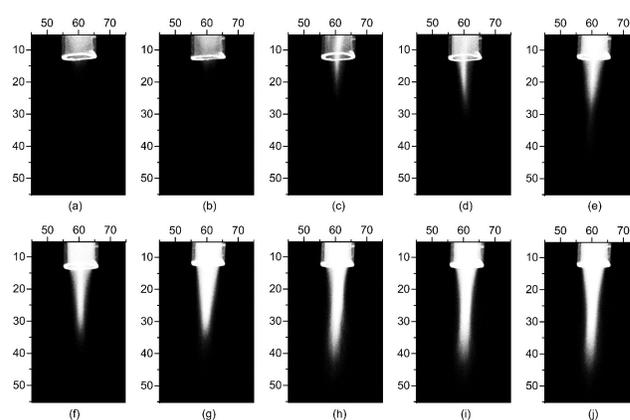
Figure 6. The length of APPJ for the 8 lit/min argon flow rate where the SDBD-like plasma jet structure is powered by repetitive high-voltage microsecond pulses ((a):25 kHz, (b):22 kHz, (c):20 kHz, (d):18 kHz, (e):16 kHz, (f):14 kHz, (g):12 kHz, (h):10 kHz. (i):8 kHz, (j):6 kHz) with low frequency sinusoidal bias.
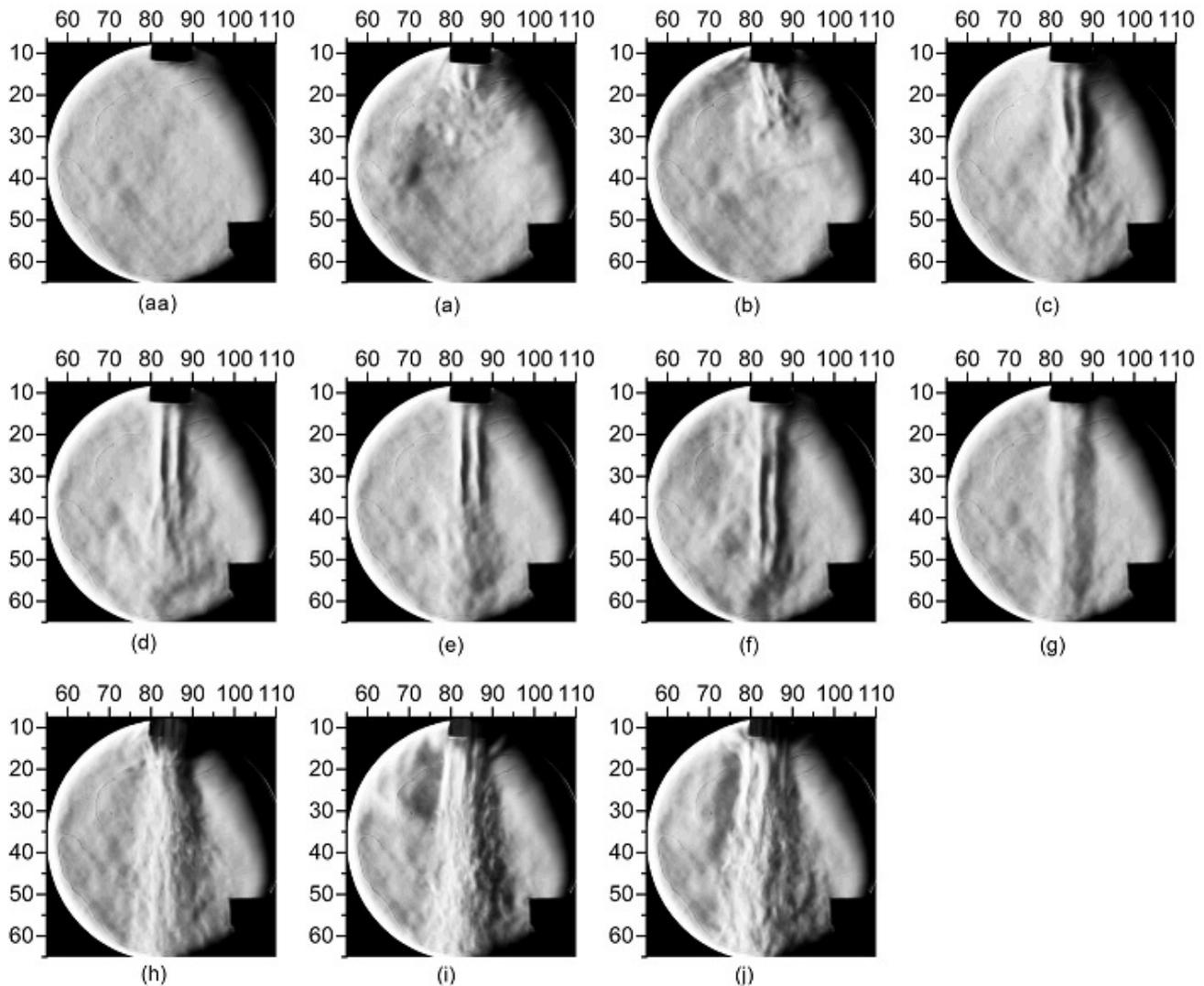
Figure 7. Schlieren images of argon plasma jet in according to the corresponding conditions of Figure 6 ((aa): Conditions without plasma).

external electric field bias [25]. In our opinion, the reason for the poor output of high frequency plasma jets may be because the total electrical power is divided between the total energy of the plasma bullets over a period of time and the observations showed that by decreasing the pulse repetition frequency, the plasma jet column becomes stronger [26]. This can be due to a decrease in the number of plasma bullets due to a decrease in frequency, followed by an increase in the energy of each plasma bullet and ultimately the strengthening of the plasma jet column [27]. Three modes were selected for surface hydrophilicity testing. Surface hydrophilicity variations are a good technique for investigating surface energy variations due to the physical and chemical effects of plasma jets on the surface. Figure 8 clearly shows that at a frequency of 6 kHz the plasma exerts energy on the surface, which reduces the contact angle of the water drop from 79 ^{o} to 7 ^{o}. The optical emission spectroscopy results in Figure 9 also confirm the mentioned

results. Spectral lines of oxygen, nitrogen, argon as well as hydroxyl radicals were observed in this spectroscopy. The intensity of these spectral lines has increased with decreasing frequency and also the surface hydrophilicity has increased significantly in these conditions.

4. Conclusion

The purpose of this study was to investigate the effect of pulse repetition frequency variations in a plasma jet similar to an S-DBD that is simultaneously amplified by an external sinusoidal electric field. In this paper, the dynamic behavior of plasma jets under the effects of varying the pulse repetition frequency with sinusoidal external bias is investigated. A single mirror-type Schlieren imaging structure was used to visualize the plasma jet flow. The advantages of mixed electric field in varying the behavior of plasma jets from laminar to turbulent and generating more homogeneous plasma jet at the
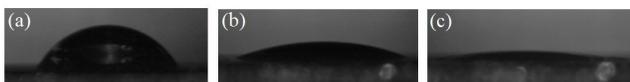
Figure 8. Contact angle of water drop on SUS (according to the corresponding conditions of Figure 6 (a):16 kHz, (b):12 kHz, (c):6 kHz).
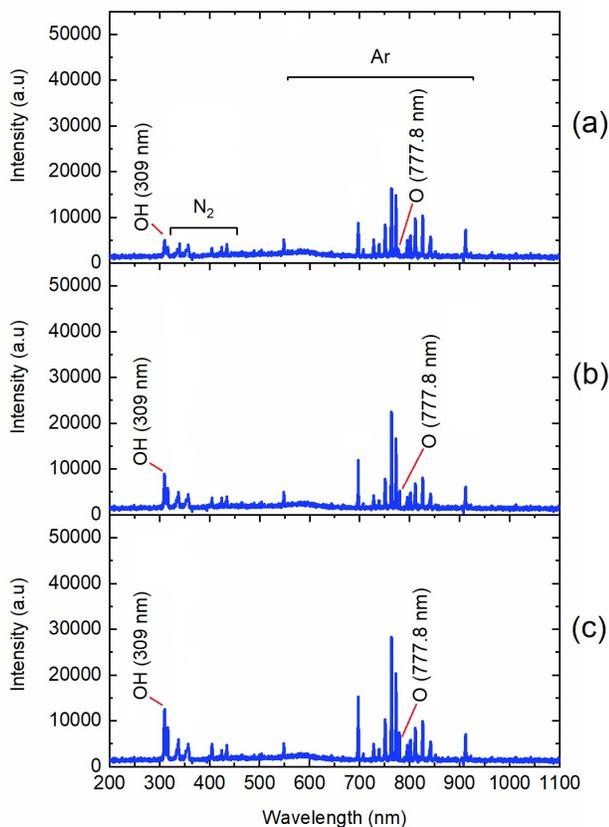
Figure 9. The OES of plasma jets at 1 cm away from the jet tube in according to the corresponding conditions of Fig 8.

output as well as increasing trend in plasma jet stability with decreasing the pulse repetition frequency are shown. These studies showed that the use of SDBD-like plasma jet structure as well as decreasing the frequency of plasma igniter pulse has an important and complementary role in surface hydrophilicity in the surface treatment process. As a final result, by using this structure, we were able to achieve a super-hydrophilic surface with equal electrical power (25 watt).

References

[1] M. Y. Naz, S. Shukrullah, S. U. Rehman, Y. Khan, A. A. Al-Arainy, and R. Meer. *Scientific Reports*, **11**:1, 2021.

[2] K. F. Sergeichev, N. A. Lukina, R. M. Sarimov, I. G. Smirnov, A. V. Simakin, A. S. Dorokhov, and S. V. Gudkov. *Front. Phys.*, **https://doi.org/10.3389/fphy.2020.614684**, 2021.

[3] Y. M. Huang, W. C. Chang, and C. L. Hsu. *Food Research International*, **141**:110108, 2021.

[4] S. Bekeschus, R. Clemen, F. Nießner, S. K. Sagwal, E. Freund, and A. Schmidt. *Advanced Science*, **7**:1903438, 2020.

[5] M. J. Nicol, T. R. Brubaker, B. J. Honish, A. N. Simmons, A. Kazemi, M. A. Geissel, C. T. Whalen, C. A. Siedlecki, S. G. Bilén, S. D. Knecht, and G. S. Kirimanjeswara. *Scientific reports*, **10**:1, 2020.

[6] A. V. Omran, G. Busco, L. Ridou, S. Dozias, C. Grillon, J. M. Pouvesle, and E. Robert. *Plasma Sources Science and Technology*, **29**:105002, 2020.

[7] P. Seyfi, A. Khademi, S. Ghasemi, A. Farhadizadeh, and H. Ghomi. *Journal of Physics D: Applied Physics*, **53**:125201, 2020.

[8] E. H. Choi. *Plasma Cancer Therapy*, **115**:53, 2020.

[9] Z. Du and X. Lin. *IOP Conference Series: Earth and Environmental Science*, **512**:012031, 2020.

[10] A. Rafiei, F. Sohbatzadeh, S. Hadavi, S. Bekeschus, M. Alimohammadi, and R. Valadan. *Clinical Plasma Medicine*, **19**:100102, 2020.

[11] K. Gazeli, T. Vazquez, G. Bauville, N. Blin-Simiand, B. Bournonville, S. Pasquiers, and J. S. Sousa. *Journal of Physics D: Applied Physics*, **53**:475202, 2020.

[12] S. Jaiswal, E. M. Aguirre, and G. V. Prakash. *Scientific Reports*, **11**:1, 2021.

[13] O. Stepanova, M. Pinchuk, A. Astafiev, and Z. Chen. *Japanese Journal of Applied Physics*, **59**:SHHC03, 2020.

[14] W. Lin, Z. Tan, X. Chen, Y. Liu, X. Wang, X. Li, and C. Sun. *IEEE Transactions on Plasma Science*, **48**:991, 2020.

[15] W. O. Younis, M. M. Berekaa, and A. H. Mohamed. *Pakistan journal of biological sciences: PJBS*, **23**:248, 2020.

[16] M. Zhang, Z. Chen, J. Wu, H. Zhang, S. Zhang, and X. Lu. *Journal of Applied Physics*, **128**:123301, 2020.

[17] J. P. Gurung, R. Shrestha, D. P. Subedi, and B. G. Shrestha. *Journal of Tropical Life Science*, **10**:149, 2020.

[18] H. B. Baniya, R. P. Guragain, B. Baniya, and D. P. Subedi. *International Journal of Polymer Science*, **2020**:1, 2020.

[19] A. A. H. Mohamed, M. M. Aljuhani, J. Q. Almarashi, and A. A. Alhazime. *Plasma Research Express*, **2**:015011, 2020.

[20] M. K. Gadzhiev, Y. M. Kulikov, E. E. Son, A. S. Tyuftyaev, M. A. Sargsyan, and D. I. Yusupov. *High Temperature*, **58**:12, 2020.

[21] R. Shrestha, D. P. Subedi, T. Niraula, M. Pokharel, P. Pandey, S. Bhattarai, J. P. Gurung, and V. P. Shrivastava. *GSJ*, **8**:1, 2020.

[22] P. Seyfi, M. R. Golghand, S. Ghasemi, and H. Ghomi. *Journal of Theoretical and Applied Physics*, **14**:195, 2020.

[23] X. Liu, H. Huang, and Y. Dai. *IEEE Sensors Journal*, **20**:9910, 2020.

[24] A. W. Gena, C. Voelker, and G. S. Settles. *Indoor air*, **30**:757, 2020.

[25] P. Seyfi, A. Heidari, A. Khademi, M. Golghand, M. Gharavi, and H. Ghomi. *Contributions to Plasma Physics*, **61**:032103, 2020.

[26] W. Lin, Z. Tan, X. Chen, Y. Liu, X. Wang, X. Li, and C. Sun. *IEEE Transactions on Plasma Science*, **48**:991, 2020.

[27] M. Hofmans, P. Viegas, O. Van Rooij, B. Klarenaar, O. Guaitella, A. Bourdon, and A. Sobota. *Plasma Sources Science and Technology*, **29**:034003, 2020.